Journal of
Synchrotron
Radiation

ISSN 0909-0495

Received 8 December 2011
Accepted 23 March 2012

Hybrid materials with an increased resistance to hard X-rays using fullerenes as radical sponges

Alessandra Pinna,[a] Luca Malfatti,[a] Massimo Piccinini,[b] Paolo Falcaro[c] and Plinio Innocenzi[a]*

[a]Laboratorio di Scienza dei Materiali e Nanotecnologie LMNT, Università di Sassari, CR-INSTM, CNBS, Palazzo Pou Salit, Piazza Duomo 6, 07041 Alghero (Sassari), Italy, [b]Porto Conte Ricerche s.r.l., SP 55, km 8400, 07041 Alghero SS, Italy, and [c]CSIRO, Division of Materials Science and Engineering, Private Bag 33, Clayton South MDC, Victoria 3169, Australia. E-mail: plinio@uniss.it

The protection of organic and hybrid organic–inorganic materials from X-ray damage is a fundamental technological issue for broadening the range of applications of these materials. In the present article it is shown that doping hybrid films with fullerenes C_{60} gives a significant reduction of damage upon exposure to hard X-rays generated by a synchrotron source. At low X-ray dose the fullerene molecules act as 'radical scavengers', considerably reducing the degradation of organic species triggered by radical formation. At higher doses the gradual hydroxylation of the fullerenes converts C_{60} into fullerol and a bleaching of the radical sinking properties is observed.

Keywords: hybrid materials; fullerene; X-ray damage; films; radical sponge.

1. Introduction

Doping of hybrid organic–inorganic materials with fullerenes and fullerene derivatives (Prato, 1997) is a well exploited route for producing different types of functional materials (Brusatin & Innocenzi, 2001; Innocenzi & Brusatin, 2001). Sol–gel chemistry has been used for introducing fullerene molecules into a large variety of oxides, mesoporous (Innocenzi *et al.*, 2004) and hybrid materials (Signorini *et al.*, 2001) to exploit the functional properties of fullerenes. In particular, non-linear optical properties of fullerenes, such as optical limiting *via* reverse saturable absorption, have allowed the production of devices for photonics. In general, fullerene derivatives have shown to be a better solution for sol–gel processing of materials, because the synthesis design can allow fullerenes to be obtained with a higher solubility and the capability of being integrated into the hybrid network *via* sol-to-gel reactions. An example are the fulleropyrrolidines which have a silicon alkoxide end-group covalently linked to the fullerene; these molecules are characterized by the presence of a solubilizing appendage together with a silicon alkoxide end-group (Maggini *et al.*, 1999). Among the different properties of fullerenes and its derivatives, two have attracted attention for developing applications (Innocenzi & Brusatin, 2001); the first one is optical limiting (Signorini *et al.*, 2001) and the second one is the capability of fullerenes to work as a radical sponge (Krusic *et al.*, 1991; McEwen *et al.*, 1992). The latter, in particular, has nowadays allowed the development of fullerene products for the market; C_{60}-based skincare cosmetics with anti-radical properties, for instance, are currently commercialized (see, for instance, products of Vitamin C_{60} BioResearch Corporation: http://www.vc60.com/). Fullerene and its derivatives have shown to be excellent antioxidant molecules and radical scavengers under UVA irradiation; this allows C_{60} and its derivatives to be used as a preventive agent for skin degradation (Xiao *et al.*, 2006). Fullerenes can sponge up and neutralize 20 or more free radicals per molecule with better performances than vitamin C and vitamin E. The radical scavenging property is due to the electronic structure of C_{60} which has several conjugated double bonds and a low-lying lowest unoccupied molecular orbital (LUMO) which can easily take up an electron, capable of reacting with radicals. This property envisages that fullerene and its derivatives could also be successfully applied to prevent plastic degradation or more in general in developing new types of UV-resistant organic materials. The radical sponge property of fullerenes could also be exploited at high energy ranges, such as the X-ray and γ-ray ranges. While the application of fullerenes to biosystems has been largely studied, so far the possibility of developing materials with enhanced capability of resistance to UV light or even higher energy radiation has almost been ignored. We have, therefore, doped a hybrid material with fullerene molecules and studied the effect upon exposure to hard X-rays produced by synchrotron radiation, quite extreme conditions for organic or hybrid materials.

2. Experimental

Phenyltriethoxysilane (PhTES), fullerene (C_{60}, 98%), hydrochloric acid (HCl) 1 *M*, 2-propanol and toluene were purchased from Aldrich and used as received; p-type boron-doped silicon wafers were employed as the substrates.

According to previous experiments (Falcaro *et al.*, 2011), the precursor sol was prepared adding 24 cm^3 of PhTES into a mixture of 48 cm^3 of toluene and 24 cm^3 of 2-propanol; after stirring for 10 min at reflux temperature (~343 K), 1.5 cm^3 of HCl 1 *M* was added dropwise. The sol was kept under stirring for 4.5 h in a flask under reflux conditions and then doped with different amounts of fullerene C_{60}. To prepare the C_{60}-doped phenylsilane coating, increasing amounts of fullerene C_{60} (1, 2.5 and 4 mg) were dispersed in 2 cm^3 of toluene; after complete solubilization by sonication, the solution appeared violet and clear. The C_{60} solutions were then added to the hydrolyzed sol and stirred for 10 min. The films were prepared by spin coating (400 rev min^{-1}) and top casting on a silicon wafer to obtain films with two different thicknesses, roughly 1.5 and 200 µm, as estimated by a digital micrometer.

Fourier-transform infrared (FTIR) measurements were performed using a Vertex 70 Bruker spectrometer in the 400–4000 cm^{-1} range with a resolution of 4 cm^{-1} on films deposited on a silicon wafer; silicon was used for background. To analyze the dataset, the spectra were cut in the 950–840 and 1420–1440 cm^{-1} regions, after which the baseline was corrected by subtracting a concave rubber-band using *OPUS 6.5* software with two iterations. The amount of residual silanol was estimated by integrating the spectra in the 950–840 cm^{-1} range after subtraction of the concave rubber-band baseline.

A Raman microscope was used to observe the formation of aggregates in the films. A Bruker Senterra confocal Raman microscope working with a laser excitation wavelength of 785 nm at 100 mW of nominal power was used for optical microscopy (100× magnification) and Raman spectroscopy analysis. The spectra were at first cut in the 1500–1420 cm^{-1} range, then a baseline was subtracted by using a concave rubber-band with ten iterations. The films were exposed to hard X-rays using the Deep X-ray Lithography beamline at the Trieste synchrotron facility (Italy). The films were irradiated with different doses by changing the exposure time (200, 400, 800 s). The films were exposed to energies per unit area incident to the sample surface corresponding to 1053.8, 2107.6 and 4215.2 J cm^{-2}. The energy per unit area is equal to the exposure time multiplied by a factor of 7.53, which is the power per unit area incident on the sample surface.

3. Results and discussion

The hybrid organic–inorganic material that we have selected is prepared using phenyltriethoxysilane as precursor, an organically modified alkoxide bearing a phenyl group which is covalently bonded to silicon; this precursor allows optically transparent and thick films to be obtained *via* spin coating or top casting. Layers several micrometres in thickness have been used to perform the experiments. Although the film is the best geometry for exposing the materials to X-rays, the detection of fullerenes in the hybrid matrix could be difficult to achieve if the coatings are not thick enough. The material has been doped with increasing amounts of fullerenes up to the solubility limit and the changes induced by X-ray exposure (Bhatta *et al.*, 2009; Weon *et al.*, 2010; Nygård *et al.*, 2010) have been studied combining FTIR and Raman spectroscopy.

The effect of X-rays on fullerene has been observed, in particular, using Raman spectroscopy because C_{60} has a quite well resolved and sharp band that can be used as a reference to check the changes induced by X-ray exposure. Fig. 1(*a*) shows the Raman spectra of samples doped with 4 mg of fullerene after exposure to hard X-rays. The samples have been exposed to increasing doses, 0 (not exposed; solid line), 1054 (dashed line), 2108 (dotted line) and 4215 J cm^{-2} (dash-dotted line). The Raman spectra of an undoped sample and pure C_{60} are also reported as a reference (Fig. 1*b*). At 1467 cm^{-1} the typical signature of the fullerene pentagonal pinching mode, Ag(2) (Kuzmany *et al.*, 2004), is clearly visible (dotted line) whereas the undoped sample does not exhibit any Raman active band in the same range (solid line). The fullerene Raman signal does not change in intensity in the samples exposed to 1054 and 2108 J cm^{-2}, whereas it is reduced to around half in the film exposed to the highest dose. Upon exposure to X-rays, a change in the Raman band has also been observed with an enlargement of the full wave half-maximum and a shift of the maximum towards lower wavenumbers. In accordance with the literature, these findings indicate a C_{60} polymerization to form dimers or trimers (Cataldo, 1993); this effect is mainly induced by the secondary electrons produced by irradiation (Klesper *et al.*, 2005; Zhao *et al.*, 1994). Upon exposure to hard X-rays, in fact, the fullerenes can be excited by secondary electrons allowing addition reactions with other C_{60} molecules.

We have then studied the effect of exposure to hard X-rays of the C_{60}-doped hybrid. Previous studies on as-deposited sol–gel films have shown that, when the sample is only partially condensed, X-rays induce polycondensation of the inorganic oxide network and degradation of the organic part (Innocenzi *et al.*, 2012). The samples are exposed to X-rays which are not monochromatic and whose energy, in accordance with the power density spectrum of the Elettra Deep X-ray Litho-

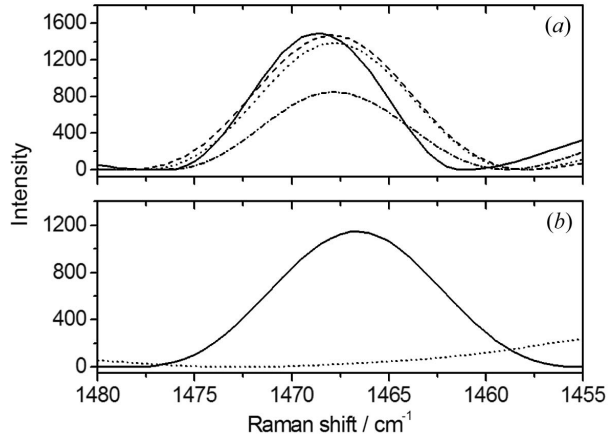

Figure 1
(*a*) Raman spectra, in the 1480–1455 cm^{-1} range, of 4 mg fullerene-doped samples after exposure to increasing X-rays doses: not-exposed (solid line), 1054 J cm^{-2} (dashed line), 2108 J cm^{-2} (dotted line) and 4215 J cm^{-2} (dash-dotted line). (*b*) Raman spectra of an undoped sample (solid line) and pure C_{60} (dotted line) in the 1480–1455 cm^{-1} range.

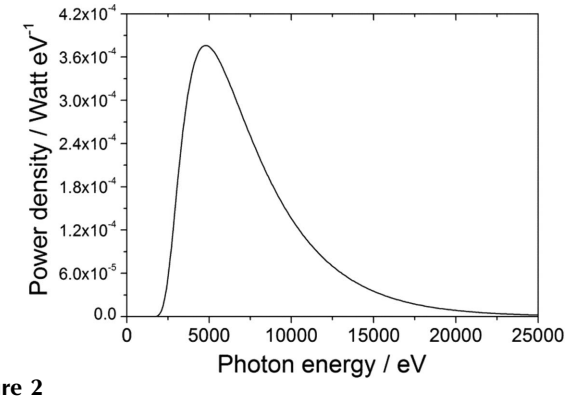

Figure 2
Power density spectrum of the Elettra Deep X-ray Lithography synchrotron beamline, ranging from 2.5 keV (upper limit of soft X-rays) to 12 keV (hard X-rays).

graphy synchrotron beamline, ranges from 2.5 keV (upper limit of soft X-rays) to 12 keV (hard X-rays) (Fig. 2). It has also to be stressed that with this energy and brilliance of the X-ray source the incident radiation is able to pass across all the sample. The penetration depth of X-rays is directly related to the absorption coefficient of the material, which is a function of wavelength (Cheng *et al.*, 1997). High-energy photons have a high penetration depth and this means that the film is homogeneously exposed to the radiation and no changes are expected between the top and bottom of the layer.

The radiation-induced effects can be successfully employed for a lithographic process on sol–gel oxides or hybrid organic–inorganic materials (Falcaro *et al.*, 2009; Costacurta *et al.*, 2010; Faustini *et al.*, 2010). Fig. 3 shows FTIR absorption spectra, in the range 950–840 cm^{-1}, of films containing different amounts of fullerenes (0 mg, dash-dotted line; 2.5 mg, dotted line; 4 mg, dashed line) and exposed to a dose of 1054 J cm^{-2} (Fig. 3*a*) and 2108 J cm^{-2} (Fig. 3*b*); the unexposed sample without fullerene (solid line) is also shown as a reference in Fig. 3(*a*). The spectra show the change of the Si–OH stretching band (Innocenzi, 2003) which is peaking at around 910 cm^{-1}, as a function of dose and fullerene concentration. The hybrid films immediately after deposition, prior to any thermal treatment, are largely uncondensed with a high amount of silanol groups; the exposure to X-rays promotes the silica condensation process through the formation of radicals. The samples exposed to the 1054 J cm^{-2} dose show, however, a quite different response, because the presence of fullerenes within the materials affects the condensation process. With respect to the undoped and exposed sample, the hybrid containing fullerenes shows a reduced condensation which means a higher content of silanols. If we compare the undoped film with the one doped with the highest content of fullerene, the amount of residual silanols appears around 65% higher; on the other hand, in comparison with the unexposed sample, some decrease in area and intensity of the band is observed. These results clearly show the radical scavenging effect of fullerenes at low X-ray doses. Under these conditions, in fact, the C_{60} molecules interact with the surrounding matter by absorbing the radical hydroxy species which are responsible for the most part of the densification and damaging of the materials

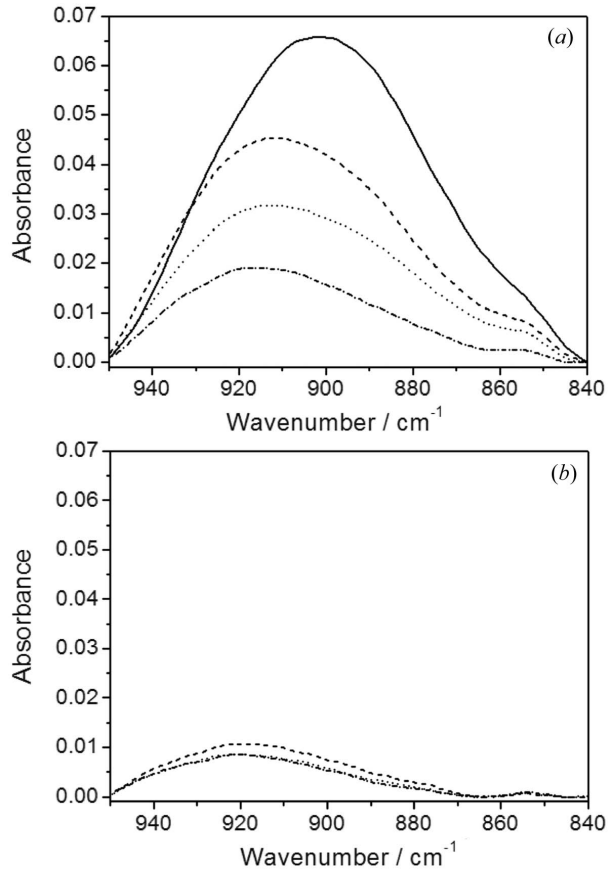

Figure 3
(*a*) FTIR absorption spectra, in the 950–840 cm^{-1} range, of phenylsilane-doped films exposed to a 1054 J cm^{-2} dose and containing decreasing amounts of C_{60} in the sol used for films deposition: 4 mg (dashed line), 2.5 (dotted line) and 0 mg (dash-dotted line). The unexposed sample without fullerene (solid line) is also shown as a reference. (*b*) FTIR absorption spectra, in the 950–840 cm^{-1} range, of phenylsilane-doped films exposed to 2108 J cm^{-2} dose and containing decreasing amounts of C_{60} in the sol used for films deposition: 4 mg (dashed line), 2.5 (dotted line) and 0 mg (dash-dotted line).

(Innocenzi *et al.*, 2011) (Fig. 4). The chemical addition of radicals produces hydroxylation of the fullerene and fullerol formation. The radical sponging, in fact, sensitively reduces the polycondensation degree of the silanols and, at the same time, the degradation of the aryl groups which are contained in the hybrid materials (see below). The samples exposed to

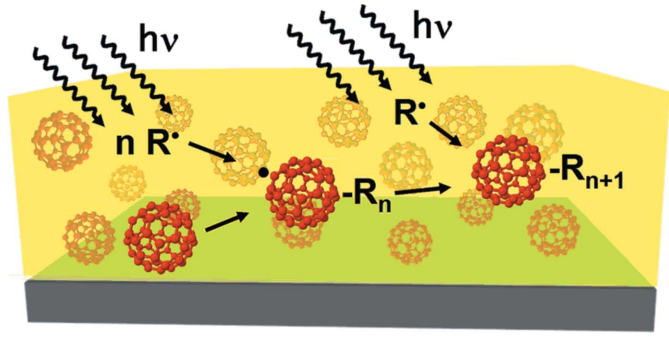

Figure 4
Hybrid materials with an increased resistance to hard X-rays using fullerenes as radical sponges.

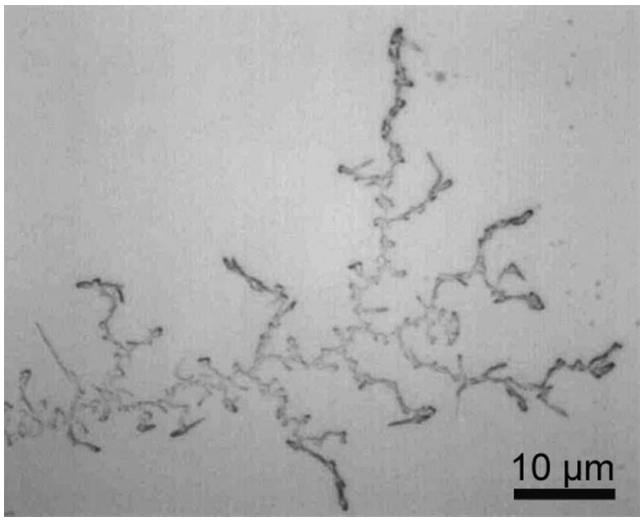

Figure 5
Optical image of 4 mg fullerene-doped films after exposure to a 2108 J cm^{-2} X-ray dose.

2108 J cm^{-2} show, instead, a different response and only a small difference in silanol content is shown by the sample doped with 4 mg of fullerene. This measure reveals that the scavenging effect depends on the concentration of fullerenes, but also that there is a saturation effect of the scavenging capability of C_{60}. At higher doses, in fact, the degree of hydroxylation of fullerenes increases up to a threshold. Under high doping conditions, the increased hydrophilicity induces the aggregation of fullerol molecules into clusters, as clearly shown in Fig. 5, in agreement with previous findings (Vileno *et al.*, 2006). The presence of aggregates has been detected only in the sample at high C_{60} doping (4 mg in the sol) exposed at doses higher than 1054 J cm^{-2}.

The effect of radiation on the organic part of the fullerene-doped hybrid material has been studied as a function of dose and C_{60} concentration by taking as reference the FTIR absorption band at 1430 cm^{-1} which is assigned to the Si-aryl band (Olejniczak *et al.*, 2005). In particular, Fig. 6(*a*) shows FTIR absorption spectra, in the 1440–1420 cm^{-1} range, of three different samples after exposure to the same dose of 1054 J cm^{-2}. The sample without fullerenes (dotted line) has the lowest absorbance which in turn increases with the content of fullerenes within the film; the absorbance in the 4 mg C_{60}-doped hybrid is double (solid line) that of the sample without fullerenes. This indicates that the presence of fullerenes reduces the organic bond cleavage owing to X-ray exposure; when a higher dose of 2108 J cm^{-2} is used, however, the radical sponge effect appears less effective (Fig. 6*b*).

The data show that fullerenes within the hybrid material behave as a radical sponge, which effectively change the response of the material upon exposure to an intense source of X-rays. By decreasing the available amount of radicals, in fact, both the inorganic polycondensation and the organic bonds cleavage are reduced. On the other hand, a careful design of the material in terms of fullerene concentration and dispersion is necessary to make the resistance of the material effective to exposure to hard X-rays.

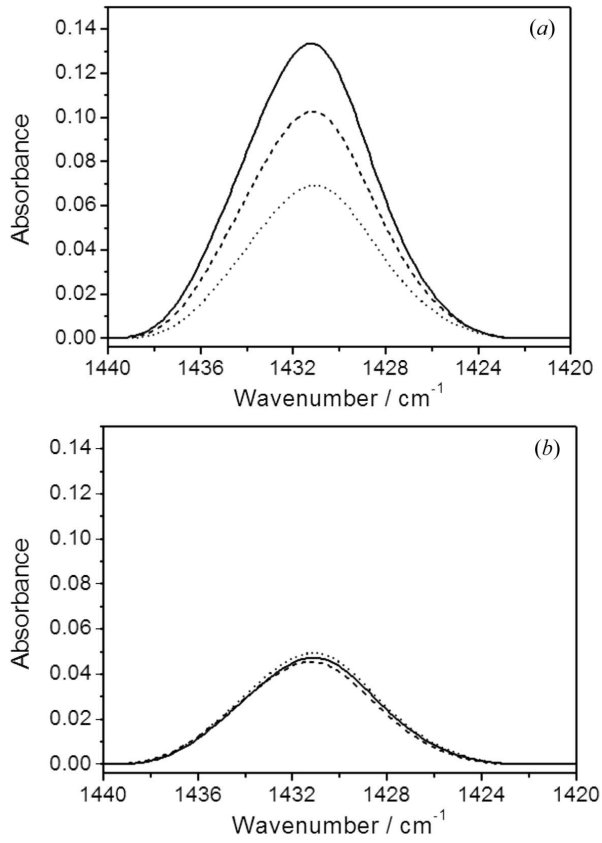

Figure 6
(*a*) FTIR absorption spectra, in the 1440–1420 cm^{-1} range, of phenylsilane-doped films exposed to a 1054 J cm^{-2} dose and containing decreasing amounts of C_{60} in the sol used for films deposition: 4 mg (solid line), 2.5 (dashed line) and 0 mg (dotted line). (*b*) FTIR absorption spectra, in the 1440–1420 cm^{-1} range, of phenylsilane-doped films exposed to a 2108 J cm^{-2} dose and containing decreasing amounts of C_{60} in the sol used for films deposition: 4 mg (solid line), 2.5 (dashed line) and 0 mg (dotted line).

4. Conclusions

The experiments, performed on C_{60} hybrid materials exposed to high-energy doses of radiation, give two main indications: (i) owing to its radical scavenging effect, fullerene enhances the resistance threshold of organic bond damage by X-rays; (ii) a radical scavenging saturation threshold exists and the concentration, dispersion and solubility of C_{60} largely affect the capability of fullerene to act as a radical sponge. Using specifically designed fullerene derivatives could allow the X-ray resistance of hybrid materials to be optimized. These experiments open the route to new classes of plastics and hybrids with the enhanced capability of resisting high-energy radiation.

Daniela Marongiu and Benedetta Marmiroli are gratefully acknowledged for experimental support.

References

Bhatta, U. M., Ghatak, J., Mukhopadhyay, M., Wang, J., Narayanan, S. & Satyam, P. V. (2009). *Nucl. Instrum. Methods Phys. Res. B*, **267**, 1807–1810.
Brusatin, G. & Innocenzi, P. (2001). *J. Sol–Gel Sci. Technol.* **22**, 189–204.

Cataldo, F. (1993). *Fullerene Sci. Technol.* **8**, 577–593.
Cheng, Y., Kuo, N.-Y. & Su, H. (1997). *Rev. Sci. Instrum.* **68**, 2163–2166.
Costacurta, S., Malfatti, L., Patelli, A., Falcaro, P., Amenitsch, H., Marmiroli, B., Grenci, G., Piccinini, M. & Innocenzi, P. (2010). *Plasma Process. Polym.* **7**, 459–465.
Falcaro, P., Costacurta, S., Malfatti, L., Buso, D., Patelli, A., Schiavuta, P., Piccinini, M., Grenci, G., Marmiroli, B., Amenitsch, H. & Innocenzi, P. (2011) *ACS Appl. Mater. Interfaces*, **3**, 245–251.
Falcaro, P., Malfatti, L., Vaccari, L., Amenitsch, H., Marmiroli, B., Grenci, G. & Innocenzi, P. (2009). *Adv. Mater.* **21**, 4932–4936.
Faustini, M., Marmiroli, B., Malfatti, L., Louis, B., Krins, N., Falcaro, P., Grenci, G., Laberty-Robert, C., Amenitsch, H., Innocenzi, P. & Grosso, D. (2010). *J. Mater. Chem.* **21**, 3597–3603.
Innocenzi, P. (2003). *J. Non-Cryst. Solids*, **316**, 309–319.
Innocenzi, P. & Brusatin, G. (2001). *Chem. Mater.* **13**, 3126–3139.
Innocenzi, P., Falcaro, P., Schergna, S., Maggini, M., Menna, E., Amenitsch, H., Grosso, D., Soler-Illia, G. J. J. A. & Sanchez, C. (2004). *J. Mater. Chem.* **14**, 1838–1842.
Innocenzi, P., Malfatti, L. & Falcaro, P. (2012). *Soft Matter*, **8**, 3722–3729.
Innocenzi, P., Malfatti, L., Kidchob, T., Costacurta, S., Falcaro, P., Marmiroli, B., Cacho-Nerin, F. & Amenitsch, H. (2011). *J. Synchrotron Rad.* **18**, 280–286.
Klesper, H., Baumann, R., Bargon, J., Hormes, J., Zumaqué-Diaz, H. & Kohring, G. A. (2005). *Appl. Phys. A*, **80**, 1469–1479.
Krusic, P. J., Wasserman, E., Keizer, P. N., Morton, J. R. & Preston, K. F. (1991). *Science*, **254**, 1183–1185.
Kuzmany, H., Pfeiffer, R., Hulman, M. & Kramberger, C. (2004). *Philos. Trans. R. Soc. London A*, **362**, 2375–2406.
McEwen, C. N., McKay, R. G. & Larsen, B. S. (1992). *J. Am. Chem. Soc.* **114**, 4412–4414.
Maggini, M., De Faveri, C., Scorrano, G., Prato, M., Brusatin, G., Guglielmi, M., Meneghetti, M., Signorini, R. & Bozio, R. (1999). *Chem. Eur. J.* **5**, 2501–2508.
Nygård, K., Gorelick, S., Vila-Comamala, J., Färm, E., Bergamaschi, A., Cervellino, A., Gozzo, F., Patterson, B. D., Ritala, M. & David, C. (2010). *J. Synchrotron Rad.* **17**, 786–790.
Olejniczak, Z., Leczka, M., Cholewa Kowalska, K., Wojtach, K., Rokita, M. & Mozgawa, W. J. (2005). *Mol. Struct.* **744–747**, 465–471.
Prato, M. (1997). *J. Mater. Chem.* **7**, 1097–1109.
Signorini, R., Tonellato, A., Meneghetti, M., Bozio, R., Prato, M., Maggini, M., Scorrano, G., Brusatin, G., Innocenzi, P. & Guglielmi, M. (2001). *J. Sol–Gel Sci. Technol.* **22**, 245–253.
Vileno, B., Marcoux, P. R., Lekka, M., Sienkiewicz, A., Fehér, T. & Forró, L. (2006). *Adv. Funct. Mater.* **16**, 120–128.
Weon, B. M., Kwon, Y. B., Won, K. H., Yoo, J., Je, J. H., Li, M. & Hahn, J. H. (2010). *Chem. Phys. Chem.* **11**, 115–118.
Xiao, L., Takada, H., Gan, X. H. & Miwa, N. (2006). *Bioorg. Med. Chem. Lett.* **16**, 1590–1595.
Zhao, Y. B., Poirier, D. M., Pechman, R. J. & Weaver, J. H. (1994). *Appl. Phys. Lett.* **64**, 577–579.